



Published in final edited form as:

*J Cell Biochem.* 2010 May ; 110(1): 44–51. doi:10.1002/jcb.22545.

## Tissue geometry patterns epithelial-mesenchymal transition via intercellular mechanotransduction

Esther W. Gomez, Qike K. Chen, Nikolce Gjorevski, and Celeste M. Nelson\*

Departments of Chemical Engineering and Molecular Biology Princeton University, Princeton, NJ 08544

### Abstract

Epithelial-mesenchymal transition (EMT) is a phenotypic change in which epithelial cells detach from their neighbors and become motile. Whereas soluble signals such as growth factors and cytokines are responsible for stimulating EMT, here we show that gradients of mechanical stress define the spatial locations at which EMT occurs. When treated with transforming growth factor (TGF)- $\beta$ , cells at the corners and edges of square mammary epithelial sheets expressed EMT markers, whereas those in the center did not. Changing the shape of the epithelial sheet altered the spatial pattern of EMT. Traction force microscopy and finite element modeling demonstrated that EMT-permissive regions experienced the highest mechanical stress. Myocardin-related transcription factor (MRTF)-A was localized to the nuclei of cells located in high-stress regions, and inhibiting cytoskeletal tension or MRTF-A expression abrogated the spatial patterning of EMT. These data suggest a causal role for tissue geometry and endogenous mechanical stresses in the spatial patterning of EMT.

### Keywords

ECM; biomechanics; force; micropatterning; mechanotransduction

### Introduction

The spatial patterning of cellular behaviors plays an important role during tissue development, differentiation, and wound healing. Localized patterns may result from a variety of stimuli, including concentration gradients of diffusible factors (morphogens), adhesion to the extracellular matrix, and mechanical forces [Nelson, 2009]. Endogenous (cell-generated) mechanical stresses arising from isometric cytoskeletal tension are transmitted within tissues between cells, their neighbors, and the surrounding extracellular matrix. In culture, gradients in mechanical stress can arise as a result of the geometry of the tissue, with free edges or areas of high curvature experiencing the greatest stress [Nelson et al., 2005]. Mechanical stress has been increasingly implicated as a key regulator of a wide range of cellular behaviors, including proliferation [Nelson et al., 2005], stem cell lineage commitment [Engler et al., 2006], and the tumorigenic phenotype [Paszek et al., 2005].

Epithelial-mesenchymal transition (EMT) is a phenotypic shift that governs a variety of morphogenetic processes, including gastrulation, neural crest development, and heart valve formation [Thiery et al., 2009]. During EMT, epithelial cells loosen attachments to their neighbors, acquire a mesenchymal-like morphology and become motile. These phenotypic

---

\*Address correspondence to CMN, A321 Engineering Quadrangle, Princeton, NJ 08544, Telephone: 609-258-8851, Fax: 609-258-0211, celesten@princeton.edu.

changes are accompanied by alterations in gene expression patterns, including attenuation of epithelial markers (such as epithelial cytokeratins and E-cadherin) and neo-expression of mesenchymal markers (such as vimentin and  $\alpha$ -smooth muscle actin ( $\alpha$ SMA)) [Zeisberg and Neilson, 2009]. Developmental EMTs occur at specific times and locations to ensure proper patterning of the embryo (reviewed in [Shook and Keller, 2003]). Pathologic EMTs can also be spatially patterned, having been observed at the edges of wounds and the invasive front of metastatic lesions [Arnoux et al., 2005; Oft et al., 1998]. EMT can be induced by soluble stimuli including cytokines, growth factors, and metalloproteinases [Thiery et al., 2009], but mechanisms for spatially patterning EMT are largely unexplored.

Here, we investigated the spatial patterning of EMT in two-dimensional (2D) sheets of epithelial cells. We found that when treated with transforming growth factor (TGF)- $\beta$ , microfabricated monolayers of mammary epithelial cells of defined shape and size underwent EMT preferentially at specific locations, notably the edges and corners of square sheets. Given that endogenous mechanical stress was concentrated in these regions, we explored how cell-cell contact and the transmission of intercellular tension affected TGF $\beta$ -induced EMT. We demonstrated that spatial patterning of EMT can result from endogenous gradients in mechanical stress, suggesting a role for the physical microenvironment in the regulation of EMT.

## Materials and Methods

### Cell culture and reagents

SCp2 mouse mammary epithelial cells were cultured as previously described [Nelson et al., 2008]. NMuMG mouse mammary epithelial cells (ATCC) were cultured in DMEM supplemented with 10% fetal bovine serum (Atlanta Biologicals), 10  $\mu$ g/mL insulin and 50  $\mu$ g/mL gentamicin. Microfabricated epithelial sheets were treated with 10 ng/mL recombinant human TGF $\beta$ 1 (R&D Systems) for 48 hours and with the following reagents: Y27632 (Tocris; 10  $\mu$ M); NSC23766 (Tocris; 100  $\mu$ M); cytochalasin D (Tocris; 200 nM); ML-7 (EMD Chemicals, 25  $\mu$ M); blebbistatin (Sigma, 25  $\mu$ M); CCG-1423 (Cayman Chemical, 10 $\mu$ M).

### Microfabrication

Microfabricated substrata containing fibronectin-coated islands were created as previously described [Nelson et al., 2008]. Briefly, poly(dimethylsiloxane) (PDMS; Ellsworth Adhesives) stamps were coated with fibronectin (BD Biosciences), rinsed in PBS, and dried under a stream of compressed nitrogen. PDMS-coated glass coverslips were UV-oxidized, stamped with fibronectin, blocked with 1% pluronics F108 (BASF), and rinsed in PBS before seeding cells. Samples were rinsed after 2 hours to remove non-adherent cells.

### Transfections and adenoviral transductions

Mouse pLKO.1 lentiviral MKL1 shRNA (shMRTF-A#1 5'-CCCACTCAGGTTCTTTCTCAA-3' and shMRTF-A#2 5'-CAGATTTCAAAGAGCCACCAT-3') were obtained from Open Biosystems. Human FLAG-tagged MRTF-A (p3xFLAG-MKL1) and pLKO.1 lentiviral scramble shRNA were obtained from Addgene. For controls, YFP was subcloned into the p3xFLAG-CMV-7.1 vector. MRTF-A- $\Delta$ N was generated using site-directed mutagenesis. Cells were transfected with plasmids using Fugene HD (Roche). Recombinant adenovirus encoding human E-cadherin lacking the  $\beta$ -catenin-binding domain (Ad-E $\Delta$ ) was a gift from Christopher Chen (University of Pennsylvania) [Nelson et al., 2005]; control adenovirus encoding GFP (Ad-GFP) was obtained from Vector Biolabs. High titer preparations of recombinant

adenoviruses were generated using the AdEasy virus purification kit (Stratagene). Cells were transduced at an MOI resulting in >99% transduction efficiency.

### Real-time PCR

Total RNA was isolated using Trizol reagent followed by cDNA synthesis using a Super Script First-Strand Synthesis kit (Invitrogen). Transcript levels were measured by quantitative real-time PCR using SYBR green chemistry. Amplification was followed by melting curve analysis to verify the presence of a single PCR product. The primers used include: 18s forward primer 5'-TCAGATACCGTCGTAGTTC-3' and reverse 5'-CCTTTAAGTTTCAGCTTTC-3'; and MRTF-A forward primer 5'-ATGGAGCTGGTGGAGAAGAATATC-3' and reverse 5'-GAAGGAGGAAGTCTGCTACC-3'.

### Immunofluorescence analysis

For staining cytoskeletal proteins, samples were fixed with 1:1 methanol:acetone at  $-20^{\circ}\text{C}$ , rinsed in PBS, blocked with 10% goat serum (Sigma), and incubated with the following primary antibodies: pan-keratin (Dako),  $\alpha$ SMA (Sigma), or vimentin (Sigma). For all other staining, samples were fixed with 4% paraformaldehyde, rinsed in PBS, permeabilized with 0.1% Triton-X-100 in PBS, blocked with 10% goat serum, and incubated with the following primary antibodies: phospho-Smad1/5/8 (Cell Signaling), TGF $\beta$ R2 (Santa Cruz),  $\beta$ -catenin (Sigma), FLAG (Sigma), or SRF (Santa Cruz). Samples were then rinsed and incubated with Alexa-conjugated secondary antibodies (Invitrogen), and nuclei were counterstained with Hoechst 33342 (Invitrogen).

### Microscopy and analysis

Samples were imaged using either a 4 $\times$  (NA = 0.2), 10 $\times$  (NA = 0.3) or 20 $\times$  (NA = 0.45) air objective on a Nikon Eclipse Ti-U inverted fluorescence microscope equipped with a Hamamatsu ORCA CCD camera. Frequency maps were created using ImageJ and Photoshop software. First, gray-scale images were converted to black-and-white images using a binarize function. Black-and-white images were then summed to create a composite gray-scale image which was converted into a color-coded frequency map using the indexed color mode in Photoshop.

### Traction forces

Finite element method (FEM) models of cell monolayers were generated as previously described [Nelson et al., 2005]. Bead displacements were measured using polyacrylamide (PA) gels. Briefly, PA gels comprised of 5% monomer and 0.03% bis-acrylamide were prepared using an adapted protocol [Pelham and Wang, 1997]. Fluorescent microbeads (1- $\mu\text{m}$  diameter, Invitrogen) were embedded in the gels and fibronectin-coated islands were stenciled onto the surface [Wang et al., 2002]. Cells were plated to confluence onto the fibronectin-coated islands, and bead locations were imaged before and after relaxation with 0.05% Triton-X-100. Displacement maps were generated using Imaris tracking software (Bitplane) and MATLAB.

## Results

### TGF $\beta$ induces EMT at the edges and corners of square epithelial sheets

TGF $\beta$ -induced EMT is characterized by down-regulation of epithelial cytokeratins and up-regulation of mesenchymal markers including vimentin and  $\alpha$ SMA. To investigate the role of tissue geometry in the spatial regulation of EMT, we used a microfabrication technique to generate confluent two-dimensional (2D) epithelial sheets of defined shape and size. SCp2

mouse mammary epithelial cells were cultured on substrata which contained 100  $\mu\text{m}$ -square fibronectin-coated islands surrounded by non-adhesive regions. When treated with TGF $\beta$ , the expression of epithelial cytokeratins decreased moderately, with a greater reduction in the cells located along the edges and corners of the square sheets (Fig. 1A,B). Conversely, de novo expression of the mesenchymal markers,  $\alpha\text{SMA}$  and vimentin, was restricted to the edges and corners of the monolayers (Fig. 1C–F). We observed no spatial differences in marker expression in the absence of treatment with TGF $\beta$  (Fig. S1). These data indicate that TGF $\beta$  induces EMT preferentially at the edges and corners of square mammary epithelial sheets, suggesting that spatial asymmetries in EMT can arise within these model tissues.

In the canonical signaling pathway, binding of TGF $\beta$  ligand to its type I (TGF $\beta$ RI) and type II (TGF $\beta$ RII) receptors stimulates phosphorylation and nuclear translocation of Smad proteins [Shi and Massague, 2003]. Spatial patterning of EMT could thus result from spatial differences in the levels of receptors or their downstream signaling. However, immunofluorescence analysis of TGF $\beta$ RII indicated that this receptor was evenly localized across the square sheets (Fig. S2). Similarly, we found even nuclear localization of phosphorylated Smad1/5/8 in sheets treated with TGF $\beta$  (Fig. S2). Thus, TGF $\beta$  signaling to the nucleus through the canonical pathway appears homogeneous across the square sheets, suggesting that the spatial patterning of EMT is due to other factors.

### **Patterned induction of EMT requires transmission of intercellular isometric tension**

Cells located along the edges of tissues simultaneously experience reduced cell-cell adhesion (due to the presence of a neighbor-free edge) and increased mechanical stress (due to propagation of isometric contractile tension) [Keller et al., 2003; Nelson et al., 2005]. Indeed, the square epithelial sheets generated gradients in endogenous mechanical stress, with cells on the corners and edges experiencing the highest magnitudes of stress [Nelson et al., 2005] (Fig. S3). Both of these microenvironmental signals have been shown to independently influence TGF $\beta$  signaling. In addition to the canonical signaling pathway, TGF $\beta$  can mediate changes in gene expression by activating any of several kinase cascades or by cooperating with cytoplasmic  $\beta$ -catenin or cytoskeletal mediators [Derynck and Zhang, 2003]. Furthermore, the ability of TGF $\beta$  to induce  $\alpha\text{SMA}$  expression in fibroblasts is regulated by cytoskeletal tension [Li et al., 2007; Tomasek et al., 2002].

To distinguish between effects due to cell-cell contact and those due to gradients of mechanical stress, we varied the geometry of the epithelial sheets. In rectangular monolayers, the TGF $\beta$ -mediated expression of  $\alpha\text{SMA}$  was concentrated on the short edges (Fig. 2A,B), regions predicted to experience the highest mechanical stress (Fig. 2C). Similarly, alterations in the expression of EMT markers were restricted to the high-stress convex regions of sinusoidal monolayers (Fig. 2D–F) as compared to the low-stress concave regions. These spatial distributions are consistent with a role for mechanical stresses in the spatial patterning of EMT markers. In epithelial sheets, gradients of mechanical stress are generated by intercellular transmission of tension from the actomyosin cytoskeleton, which is regulated in part by signaling through RhoA, its effector Rho kinase (ROCK), and myosin light chain kinase (MLCK). Decreasing contractile tension through treatment with the ROCK inhibitor Y27632, the MLCK inhibitor ML-7, or the non-muscle myosin ATPase inhibitor blebbistatin all reduced the number of epithelial sheets exhibiting spatial patterning of EMT markers (Fig. 2G). Although other Rho family GTPases can affect tissue contractility, inhibiting signaling through Rac by treatment with NSC23766 disrupted formation of lamellipodia but had no effect on TGF $\beta$ -induced patterning of EMT (Fig. S4).

Cells within sheets transmit tension to and from their neighbors through cadherin-mediated intercellular adhesions [Adams and Nelson, 1998]. To determine whether the spatial patterning of EMT is directed by intercellular transmission of cytoskeletal tension, we

infected cells with recombinant adenovirus containing a cytoplasmic deletion mutant of E-cadherin (Ad-E $\Delta$ ) that blocks the connection between E-cadherin and the actin cytoskeleton by inhibiting junctional localization of  $\beta$ -catenin [Nelson et al., 2005] (Fig. 3A,B). Immunofluorescence staining revealed that TGF $\beta$  induced spatially uniform expression of  $\alpha$ SMA within E $\Delta$ -expressing sheets, as compared to patterned expression of  $\alpha$ SMA observed in control sheets infected with adenovirus containing GFP (Ad-GFP) (Fig. 3C–F). These data are consistent with the spatial patterning of EMT being regulated by intercellular tension.

### Tissue geometry patterns EMT by governing the nuclear localization of MRTF-A

In addition to signaling through Smads, TGF $\beta$  has been demonstrated to enhance binding of serum response factor (SRF) to CA $\alpha$ G boxes within the promoter regions of genes including  $\alpha$ SMA [Hautmann et al., 1999]. SRF regulates the transcription of many genes involved in proliferation and differentiation, including immediate early genes and actin-regulatory proteins (reviewed by [Posern and Treisman, 2006]). A subgroup of SRF-target genes is sensitive to Rho-actin signaling; this differential control is mediated by the SRF cofactors, myocardin-related transcription factors (MRTF)-A and -B (also known as MAL and MKL1/2) [Miralles et al., 2003]. MRTF-A regulates the transcription of  $\alpha$ SMA [Elberg et al., 2008] and was also recently shown to effect TGF $\beta$ -mediated EMT by associating with Smad3 to enhance the transcription of Slug [Morita et al., 2007]. Immunofluorescence analysis revealed that nuclear localization of SRF was evenly distributed across the epithelial sheets (Fig. S5). However, we found patterned nuclear localization of FLAG-tagged MRTF-A along the edges and corners (Fig. 4A,B). The patterned nuclear localization of MRTF-A was correlated with patterned  $\alpha$ SMA expression in these epithelial sheets (Fig. 4C). Down-regulating the expression of MRTF-A with shRNA reduced the number of epithelial sheets exhibiting patterned  $\alpha$ SMA expression in comparison to controls (Fig. 4D,E). Furthermore, treatment with CCG-1423, which inhibits the interaction between SRF and MRTF-A [Evelyn et al., 2007], decreased TGF $\beta$ -mediated EMT (Fig. 2G). These data suggest that TGF $\beta$  induces patterned EMT by cooperating with SRF/MRTF-A.

The activity and nuclear localization of MRTF-A are regulated by its association with monomeric G-actin [Asparuhova et al., 2009; Posern and Treisman, 2006]. Increased cytoskeletal tension causes nuclear translocation of MRTF-A by reducing the available pool of monomeric actin [Posern and Treisman, 2006]. Consistent with the localization patterns, treatment with cytochalasin D, which drives MRTF-A into the nucleus by disrupting its association with actin monomers [Busche et al., 2008], resulted in EMT over the entire surface of the epithelial sheets (Fig. S6). Conversely, over-expressing a constitutively active form of MRTF-A (MRTF-A- $\Delta$ N), which lacks the RPEL motifs responsible for binding to actin monomers [Busche et al., 2008; Miralles et al., 2003], resulted in unpatterned nuclear localization of MRTF-A. MRTF-A- $\Delta$ N-expressing monolayers treated with TGF $\beta$  showed expression of  $\alpha$ SMA over the entire epithelial sheet (Fig. 4F–H). These data suggest that tissue geometry patterns EMT by regulating the nuclear localization of MRTF-A.

## Discussion

In this study, we found that spatial patterns of EMT can arise within epithelial sheets and that the patterning is consistent with gradients of mechanical stress sculpted by tissue geometry. We observed similar results in TGF $\beta$ -treated monolayers of NMuMG mouse mammary epithelial cells (Fig. S7), a widely used model for EMT. Gradients of mechanical stress have previously been reported to yield spatial asymmetries in a diverse array of cellular behaviors, including proliferation [Nelson et al., 2005], motility [Parker et al., 2002], and stem cell differentiation [Ruiz and Chen, 2008]. Our results may give insight into the mechanisms by which mechanical stress is transduced into these phenotypes. Here,

TGF $\beta$ -mediated EMT is controlled by patterns of nuclear localization of the SRF cofactor, MRTF-A. SRF is a widely expressed transcription factor responsible for regulating a plethora of genes involved in cell proliferation and differentiation. Actin cytoskeletal dynamics modulated by Rho family GTPases control the localization of MRTF-A, which in turn controls binding of SRF to CA $\alpha$ G boxes in the promoters of responsive genes. Given the recently uncovered links between EMT and stem cell differentiation [Mani et al., 2008], it will be interesting to determine whether Rho-mediated mechanical gradients influence both differentiation programs through MRTF-A.

Previous studies have implicated contact disassembly in the nuclear accumulation of MRTF-A and subsequent EMT [Busche et al., 2008; Fan et al., 2007; Masszi et al., 2004; Sebe et al., 2008]. Our data suggest that loss of cell-cell contact per se is not sufficient for nuclear translocation of MRTF-A and induction of EMT in monolayers of mammary epithelial cells. That is, not all cells located at the edges of monolayers undergo EMT. The edges refractory to the EMT stimulus are those predicted to be located in the low-stress regions of the monolayer, suggesting that nuclear translocation of MRTF-A is co-regulated by cell-cell contacts (or the lack thereof) and isometric tension within the tissue. This interpretation is validated by previous studies which found that applying exogenous forces induced  $\alpha$ SMA expression in fibroblasts [Chan et al., 2009; Zhao et al., 2007], whereas inhibiting isometric tension prevented EMT in sub-confluent cultures of kidney tubular cells [Fan et al., 2007]. These data also suggest that edge-free regions of tissues (such as three-dimensional tissues *in vivo*) that experience high mechanical stress may also show enhanced EMT.

A number of cytokines and other soluble stimuli can induce EMT during normal and pathological development. Our data add to the growing evidence suggesting a role for the physical microenvironment in the regulation of EMT. Insoluble ECM molecules within the microenvironment impart signaling information and control cell morphology. Indeed, ECM components can regulate EMT in some cell lines [Shintani et al., 2008], and cell morphology regulates the induction of EMT by matrix metalloproteinase-3 [Nelson et al., 2008]. The size and shape of a tumor control the distribution of oxygen within its mass; tumorigenic EMT is affected profoundly by hypoxia (reviewed by [Hill et al., 2009]). Furthermore, spatial segregation of EMT has been observed at the edges of healing wounds [Arnoux et al., 2005] and the leading edge of invasive metastatic cohorts [Brabletz et al., 2001; Oft et al., 1998]. This patterning may be due to geometrically-prescribed intercellular tension such as described here. Dissecting how EMT is patterned may thus help to reveal the mechanisms involved in normal and metastatic development.

## Supplementary Material

Refer to Web version on PubMed Central for supplementary material.

## Acknowledgments

**Funded by:** • National Institutes of Health (NIH); Grant Numbers: CA128660 and GM083997

• Susan G. Komen for the Cure; Grant Number: FAS0703855

We would like to thank L. Loo for use of her cleanroom and K. Lee, C. Liu, and A. Pavlovich for technical assistance. This work was supported in part by grants from the NIH (CA128660 and GM083997), Susan G. Komen for the Cure (FAS0703855), and the David and Lucile Packard Foundation. C.M.N. holds a Career Award at the Scientific Interface from the Burroughs Wellcome Fund. E.W.G. was supported by postdoctoral fellowships from the New Jersey Commission on Cancer Research and Susan G. Komen for the Cure.

## Abbreviations

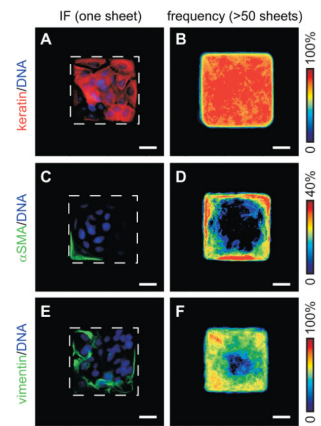
<b>EMT</b>	epithelial-mesenchymal transition
<b>FEM</b>	finite element method
<b>MRTF</b>	myocardin-related transcription factor
<b>SMA</b>	smooth muscle actin
<b>SRF</b>	serum response factor
<b>TGF</b>	transforming growth factor
<b>TGF<math>\beta</math>RII</b>	TGF $\beta$ receptor type II
<b>2D</b>	two-dimensional

## References

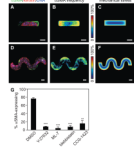
- Adams CL, Nelson WJ. Cytomechanics of cadherin-mediated cell-cell adhesion. *Curr Opin Cell Biol.* 1998; 10:572–7. [PubMed: 9818166]
- Arnoux, V.; Come, C.; Kusewitt, D.; Hudson, L.; Savagner, P. Cutaneous wound reepithelialization: a partial and reversible EMT. In: Savagner, P., editor. *Rise and fall of epithelial phenotype: concepts of epithelial-mesenchymal transition.* Berlin: Springer; 2005. p. 111-134.
- Asparuhova MB, Gelman L, Chiquet M. Role of the actin cytoskeleton in tuning cellular responses to external mechanical stress. *Scand J Med Sci Sports.* 2009; 19:490–9. [PubMed: 19422655]
- Brabletz T, Jung A, Reu S, Porzner M, Hlubek F, Kunz-Schughart LA, Knuechel R, Kirchner T. Variable beta-catenin expression in colorectal cancers indicates tumor progression driven by the tumor environment. *Proc Natl Acad Sci U S A.* 2001; 98:10356–61. [PubMed: 11526241]
- Busche S, Descot A, Julien S, Genth H, Posern G. Epithelial cell-cell contacts regulate SRF-mediated transcription via Rac-actin-MAL signalling. *J Cell Sci.* 2008; 121:1025–35. [PubMed: 18334560]
- Chan MW, Arora PD, Bozavikov P, McCulloch CA. FAK, PIP5KI $\{\gamma\}$  and gelsolin cooperatively mediate force-induced expression of  $\{\alpha\}$ -smooth muscle actin. *J Cell Sci.* 2009; 122:2769–81. [PubMed: 19596799]
- Derynck R, Zhang YE. Smad-dependent and Smad-independent pathways in TGF-beta family signalling. *Nature.* 2003; 425:577–84. [PubMed: 14534577]
- Elberg G, Chen L, Elberg D, Chan MD, Logan CJ, Turman MA. MKL1 mediates TGF-beta1-induced alpha-smooth muscle actin expression in human renal epithelial cells. *Am J Physiol Renal Physiol.* 2008; 294:F1116–28. [PubMed: 18337547]
- Engler AJ, Sen S, Sweeney HL, Discher DE. Matrix elasticity directs stem cell lineage specification. *Cell.* 2006; 126:677–89. [PubMed: 16923388]
- Evelyn CR, Wade SM, Wang Q, Wu M, Iniguez-Lluhi JA, Merajver SD, Neubig RR. CCG-1423: a small-molecule inhibitor of RhoA transcriptional signaling. *Mol Cancer Ther.* 2007; 6:2249–60. [PubMed: 17699722]
- Fan L, Sebe A, Peterfi Z, Masszi A, Thirone AC, Rotstein OD, Nakano H, McCulloch CA, Szaszi K, Mucsi I, Kapus A. Cell contact-dependent regulation of epithelial-myofibroblast transition via the rho-rho kinase-phospho-myosin pathway. *Mol Biol Cell.* 2007; 18:1083–97. [PubMed: 17215519]
- Hautmann MB, Adam PJ, Owens GK. Similarities and differences in smooth muscle alpha-actin induction by TGF-beta in smooth muscle versus non-smooth muscle cells. *Arterioscler Thromb Vasc Biol.* 1999; 19:2049–58. [PubMed: 10479645]
- Hill RP, Marie-Egyptienne DT, Hedley DW. Cancer stem cells, hypoxia and metastasis. *Semin Radiat Oncol.* 2009; 19:106–11. [PubMed: 19249648]
- Keller R, Davidson LA, Shook DR. How we are shaped: the biomechanics of gastrulation. *Differentiation.* 2003; 71:171–205. [PubMed: 12694202]

- Li Z, Dranoff JA, Chan EP, Uemura M, Seigny J, Wells RG. Transforming growth factor-beta and substrate stiffness regulate portal fibroblast activation in culture. *Hepatology*. 2007; 46:1246–56. [PubMed: 17625791]
- Mani SA, Guo W, Liao MJ, Eaton EN, Ayyanan A, Zhou AY, Brooks M, Reinhard F, Zhang CC, Shipitsin M, Campbell LL, Polyak K, Brisken C, Yang J, Weinberg RA. The epithelial-mesenchymal transition generates cells with properties of stem cells. *Cell*. 2008; 133:704–15. [PubMed: 18485877]
- Masszi A, Fan L, Rosivall L, McCulloch CA, Rotstein OD, Mucsi I, Kapus A. Integrity of cell-cell contacts is a critical regulator of TGF-beta 1-induced epithelial-to-myofibroblast transition: role for beta-catenin. *Am J Pathol*. 2004; 165:1955–67. [PubMed: 15579439]
- Miralles F, Posern G, Zaromytidou AI, Treisman R. Actin dynamics control SRF activity by regulation of its coactivator MAL. *Cell*. 2003; 113:329–42. [PubMed: 12732141]
- Morita T, Mayanagi T, Sobue K. Dual roles of myocardin-related transcription factors in epithelial mesenchymal transition via slug induction and actin remodeling. *J Cell Biol*. 2007; 179:1027–42. [PubMed: 18056415]
- Nelson CM. Geometric control of tissue morphogenesis. *Biochim Biophys Acta*. 2009; 1793:903–10. [PubMed: 19167433]
- Nelson CM, Jean RP, Tan JL, Liu WF, Sniadecki NJ, Spector AA, Chen CS. Emergent patterns of growth controlled by multicellular form and mechanics. *Proc Natl Acad Sci U S A*. 2005; 102:11594–9. [PubMed: 16049098]
- Nelson CM, Khauv D, Bissell MJ, Radisky DC. Change in cell shape is required for matrix metalloproteinase-induced epithelial-mesenchymal transition of mammary epithelial cells. *J Cell Biochem*. 2008; 105:25–33. [PubMed: 18506791]
- Oft M, Heider KH, Beug H. TGFbeta signaling is necessary for carcinoma cell invasiveness and metastasis. *Curr Biol*. 1998; 8:1243–52. [PubMed: 9822576]
- Parker KK, Brock AL, Brangwynne C, Mannix RJ, Wang N, Ostuni E, Geisse NA, Adams JC, Whitesides GM, Ingber DE. Directional control of lamellipodia extension by constraining cell shape and orienting cell tractional forces. *Faseb J*. 2002; 16:1195–204. [PubMed: 12153987]
- Paszek MJ, Zahir N, Johnson KR, Lakins JN, Rozenberg GI, Gefen A, Reinhart-King CA, Margulies SS, Dembo M, Boettiger D, Hammer DA, Weaver VM. Tensional homeostasis and the malignant phenotype. *Cancer Cell*. 2005; 8:241–54. [PubMed: 16169468]
- Pelham RJ Jr, Wang Y. Cell locomotion and focal adhesions are regulated by substrate flexibility. *Proc Natl Acad Sci U S A*. 1997; 94:13661–5. [PubMed: 9391082]
- Posern G, Treisman R. Actin' together: serum response factor, its cofactors and the link to signal transduction. *Trends Cell Biol*. 2006; 16:588–96. [PubMed: 17035020]
- Ruiz SA, Chen CS. Emergence of Patterned Stem Cell Differentiation within Multicellular Structures. *Stem Cells*. 2008; 26:2921–2927. [PubMed: 18703661]
- Sebe A, Masszi A, Zulys M, Yeung T, Speight P, Rotstein OD, Nakano H, Mucsi I, Szaszi K, Kapus A. Rac, PAK and p38 regulate cell contact-dependent nuclear translocation of myocardin-related transcription factor. *FEBS Lett*. 2008; 582:291–8. [PubMed: 18154735]
- Shi Y, Massague J. Mechanisms of TGF-beta signaling from cell membrane to the nucleus. *Cell*. 2003; 113:685–700. [PubMed: 12809600]
- Shintani Y, Maeda M, Chaika N, Johnson KR, Wheelock MJ. Collagen I promotes epithelial-to-mesenchymal transition in lung cancer cells via transforming growth factor-beta signaling. *Am J Respir Cell Mol Biol*. 2008; 38:95–104. [PubMed: 17673689]
- Shook D, Keller R. Mechanisms, mechanics and function of epithelial-mesenchymal transitions in early development. *Mech Dev*. 2003; 120:1351–83. [PubMed: 14623443]
- Thiery JP, Acloque H, Huang RY, Nieto MA. Epithelial-mesenchymal transitions in development and disease. *Cell*. 2009; 139:871–890. [PubMed: 19945376]
- Tomasek JJ, Gabbiani G, Hinz B, Chaponnier C, Brown RA. Myofibroblasts and mechano-regulation of connective tissue remodelling. *Nat Rev Mol Cell Biol*. 2002; 3:349–63. [PubMed: 11988769]
- Wang N, Ostuni E, Whitesides GM, Ingber DE. Micropatterning tractional forces in living cells. *Cell Motil Cytoskeleton*. 2002; 52:97–106. [PubMed: 12112152]

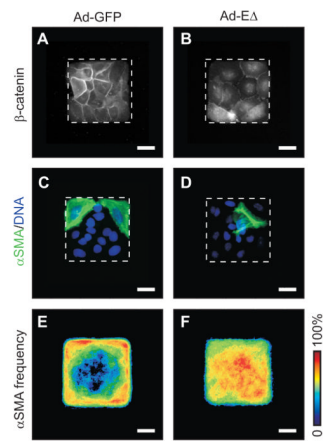
- Zeisberg M, Neilson EG. Biomarkers for epithelial-mesenchymal transitions. *J Clin Invest.* 2009; 119:1429–37. [PubMed: 19487819]
- Zhao XH, Laschinger C, Arora P, Szaszi K, Kapus A, McCulloch CA. Force activates smooth muscle alpha-actin promoter activity through the Rho signaling pathway. *J Cell Sci.* 2007; 120:1801–9. [PubMed: 17456553]



**Fig. 1.** TGF $\beta$  induces spatial patterning of EMT in 2D epithelial sheets. Immunofluorescence staining and frequency maps for (A,B) cytokeratins, (C,D)  $\alpha$ SMA, and (E,F) vimentin for TGF $\beta$ -treated tissues. Scale bars, 25  $\mu$ m.



**Fig. 2.** Spatial patterning of EMT correlates with endogenous gradients of cytoskeletal tension. **(A)** Immunofluorescence staining and **(B)** frequency map for  $\alpha$ SMA expression in rectangular epithelial sheets treated with TGF $\beta$ . **(C)** Sites of EMT correlate with FEM-predicted endogenous mechanical stress. **(D)** Immunofluorescence staining and **(E)** frequency map for  $\alpha$ SMA expression, and **(F)** FEM-predicted distribution of mechanical stress in sinusoidal epithelial sheets treated with TGF $\beta$ . **(G)** Frequency of epithelial sheets with patterned  $\alpha$ SMA expression after simultaneous treatment with TGF $\beta$  and DMSO vehicle, Y27632, ML-7, blebbistatin, or CCG-1423. Scale bars, 50  $\mu$ m. (\*\*),  $p < 0.005$ ; (\*\*\*),  $p < 0.0001$  compared to DMSO.

**Fig. 3.**

Spatial patterning of EMT arises from intercellular transmission of stress.

Immunofluorescence staining for  $\beta$ -catenin in epithelial sheets transduced with (A) Ad-GFP or (B) Ad-E $\Delta$ . Immunofluorescence staining for  $\alpha$ SMA (green) and DNA (blue) in epithelial sheets transduced with (C) Ad-GFP or (D) Ad-E $\Delta$  and simultaneously treated with TGF $\beta$ . Frequency maps of  $\alpha$ SMA expression in epithelial sheets transduced with (E) Ad-GFP or (F) Ad-E $\Delta$  and simultaneously treated with TGF $\beta$ . Scale bars, 25  $\mu$ m.

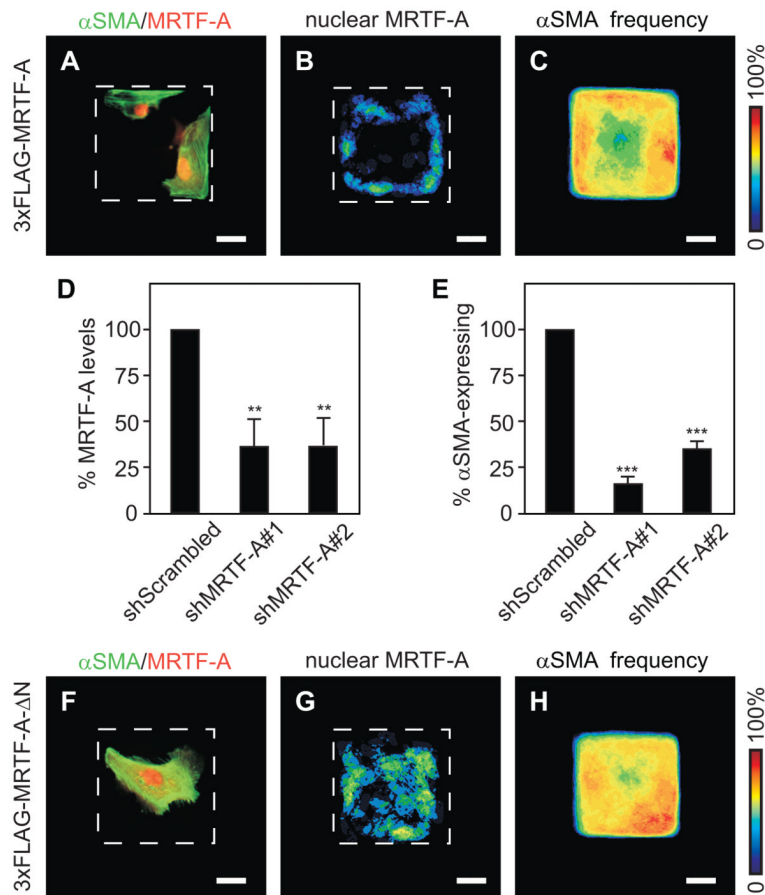


**Fig. 4.** Spatial patterning of the nuclear localization of MRTF-A governs spatial patterning of EMT. Nuclear localization of FLAG-tagged MRTF-A correlates with  $\alpha$ SMA expression. Shown are (A) immunofluorescence staining for  $\alpha$ SMA (green) and FLAG (red), (B) frequency map of nuclear FLAG-tagged MRTF-A, and (C) frequency map of  $\alpha$ SMA expression in FLAG-tagged MRTF-A-expressing sheets treated with TGF $\beta$ . Down-regulating MRTF-A expression blocks patterned EMT. Shown are (D) transcript levels of MRTF-A for cells transfected with shRNA and (E) frequency of shRNA-transfected epithelial sheets with patterned  $\alpha$ SMA expression after treatment with TGF $\beta$ . Forced nuclear localization of MRTF-A disrupts patterned EMT. Shown are (F) immunofluorescence staining for  $\alpha$ SMA (green) and FLAG (red), (G) frequency map of nuclear FLAG-tagged MRTF-A- $\Delta$ N, and (H) frequency map of  $\alpha$ SMA expression in FLAG-tagged MRTF-A- $\Delta$ N-expressing sheets treated with TGF $\beta$ . Scale bars, 25  $\mu$ m. (\*\*),  $p < 0.05$ ; (\*\*\*),  $p < 0.005$  compared to shScrambled.